Machine Learning-Aided Trajectory Prediction and Conflict Detection for Internet of Aerial Vehicles

Cheng Cheng, *Graduate Student Member, IEEE*, Liang Guo, Tong Wu, Jinlong Sun, *Member, IEEE*, Guan Gui, *Senior Member, IEEE*, Bamidele Adebisi, *Senior Member, IEEE*, Haris Gacanin, *Fellow, IEEE*, and Hikmet Sari, *Life Fellow, IEEE*

***Abstract*—As exploitation of low and medium airspace for air traffic management (ATM) is gaining more attention, aerial vehicles' security issues pose a major challenge to the Air-Ground Integrated Vehicle Networks (AGIVN). Traditional surveillance technology lacks the capacity to support the intensive air traffic management (ATM) of the future. Therefore, an advanced automatic dependent surveillance-broadcast (ADS-B) technique is applied to track and monitor aerial vehicles in a more effective manner. In this paper, we propose a grouping-based conflict detection algorithm based on the preprocessed ADS-B dataset, and analyze the experimental results and visualize the detected conflicts. Then, in order to further improve flight safety and conflict detection, the trajectories of the aerial vehicles are predicted based on machine learning-based algorithms. The results are fed into the conflict detection algorithm to execute conflict prediction. It was shown that the trajectory prediction model using long short-term memory (LSTM) can achieve better prediction performance, especially when predicting the long-term trajectory of aerial vehicles. And the conflict detection results based on the trajectory prediction methods show that the proposed scheme can make it possible to detect whether there would be conflicts within seconds.**

***Index Terms*—Conflict detection, automatic dependent surveillance-broadcast (ADS-B), trajectory prediction, machine learning, aerial vehicle.**

I. Introduction

Future sixth-generation wireless network outlines a cellular-free multi-layer network that integrates space, air, ground and underwater communications [1]. Internet of aerial vehicles plays a role in air communications. Compared with space and underwater communications, it shows flexibility in deployment, scheduling and maintenance. Hence, Internet of aerial vehicles is an important part of future Internet of everything (IoE), and new applications of air-ground integrated vehicular networks (AGIVN) can provide golden opportunities for traditional and emerging enterprises.

With the opening of low-altitude airspace, AGIVN covering drones, helicopters, and unmanned free balloons are developing rapidly [2]–[4]. As a result, the low and medium airspaces are becoming crowded, and security pose higher requirements for the AGIVN. According to civil aviation administration of China, more than 90% of accidents have occurred at low altitudes since the 21st century. Therefore, new techniques need be utilized to reduce probability of aerial vehicles collisions [5].

Traditional surveillance technologies, such as primary surveillance radars and secondary surveillance radars [6]–[8], have obvious technical limitations in meeting requirements of future dense air traffic management (ATM) such as high operating costs, limited coverage, and relatively low accuracy of tracking [9]–[11]. To address these challenges, an automatic dependent surveillance-broadcast (ADS-B) technique has been proposed to enhance the surveillance architecture [12]–[14]. In the future AGIVN and IoE, the ADS-B technique can play an important role to facilitate the management of aerial resources in an intelligent manner [15]. Traditional conflict detection and collision avoidance algorithms often rely on collaborative systems (e.g., traffic collision avoidance system (TCAS) [16]), or non-cooperative systems (e.g., stand-alone photoelectric sensors and airborne radars used for obstacle detection [17]). However, information provided by the TCAS and radars is generally two-dimensional and the maintenance cost is relatively high [18], [19]. Nevertheless, ADS-B messages obtained from the distributed ADS-B stations can provide a wealth of aerial vehicles-related information, and the maintenance cost of the ADS-B stations is much lower.

To determine whether there is a conflict alarm between arbitrary two aerial vehicles. G. Xiao *et al*. [20] divided the space around an aerial vehicle into four quadrants. Based on the four quadrants, the relative position, speed, and angle are compared with other aerial vehicles to determine whether there exists conflicts. B. Zhou *et al*. divided the three-dimensional area centered on the evaluated aerial vehicle into 26 areas, including 8 hexagram areas, 6 axial areas, and 12 quadrant areas [21]. The correlation between an invading aerial vehicle and the evaluated aerial vehicle is determined by the area where the invading aerial vehicle is located.

This work was supported by the Major Project of the Ministry of Industry and Information Technology of China under Grant TC190A3WZ-2, National Natural Science Foundation of China under Grant 61901228, the Six Top Talents Program of Jiangsu under Grant XYDXX-010, the 1311 Talent Plan of Nanjing University of Posts and Telecommunications *(Corresponding authors: Jinlong Sun, Guan Gui, and Hikmet Sari).*

Cheng Cheng, Jinlong Sun, Guan Gui, and Hikmet Sari are with the College of Telecommunications and Information Engineering, Nanjing University of Posts and Telecommunications, Nanjing 210003, China (e-mails: {1019010402, sunjinlong, guiguan, hikmet}@njupt.edu.cn).

Liang Guo is with the Institute for Cloud Computing and Big Data, China Academy of Information and Communications Technology, Beijing 100191, China (e-mail: guoliang1@caict.ac.cn).

Tong Wu is with the National Institute of Metrology, Beijing 100029, China (e-mail: wut@nim.ac.cn).

Bamidele Adebisi is with the Department of Engineering, Faculty of Science and Engineering, Manchester Metropolitan University, Manchester M1 5GD, United Kingdom (e-mail: b.adebisi@mmu.ac.uk).

Haris Gacanin is with the Institute for Communication Technologies and Embedded Systems, RWTH Aachen University, Aachen 52062, Germany (e-mail: E-mail: harisg@ice.rwth-aachen.de).

However, the position of the aerial vehicle is time-varying and dynamic, making the relative relationship between the invading aerial vehicle and the evaluated aerial vehicle also dynamic. Therefore, these algorithms using segmented areas to detect aerial vehicles conflicts are generally not real-time. In order to solve the above problems, an ADS-B based conflict detection scheme using a grouping strategy is proposed in this paper. The conflict detection algorithm is motivated by the time axis mapping algorithm [22]. First, the route conflict problem is converted into a three-dimensional coordinate (X, Y, Z) conflict problem, and the conflict area of the three-dimensional coordinate axis is uniformly mapped onto the time axis. The route conflict of the two aerial vehicles is determined by determining whether there is an intersection of the X, Y, and Z axes at the same time period. Here, the grouping strategy is utilized to divide multi-dimensional information [23] (including longitude, latitude, altitude, ground speed, vertical speed, heading angle, etc.) of all aerial vehicles at the same time into multiple small groups. By using the multiple small groups, the complexity and execution time of the conflict detection system can be notably reduced.

Although an aerial vehicle has a flight plan in advance, there could be a difference between the actual flight and the plan, and the error can be about 7km [24]. Hence, an aerial vehicle often fails to fly as scheduled, it often conflicts with other aerial vehicles. Hence, although there is a flight plan, it is still necessary to predict the trajectories of aerial vehicles. In order to further improve the safety and advancement of the conflict detection algorithm, this paper combines a long short-term memory (LSTM) [25], [26] based trajectory prediction method with the conflict prediction algorithm. In this way, the predicted trajectory information can be used to make conflict detection for future seconds, and can prepare for collision avoidance in advance. The contributions of this paper can be summarized as follows:

- A geometric model for detecting whether an aerial vehicle is in conflict is constructed, and a grouping-based aerial vehicle conflicts detection algorithm is proposed.
- To improve the safety of the conflict detection algorithm, it is combined with three machine learning-based methods, i.e., LSTM, convolutional neural networks (CNN) and least square (LS), which are used and compared in predicting the short-term and long-term trajectories of the aerial vehicles.
- To address the real conflict situations, we discuss the impact of the trajectory prediction accuracy on the conflict prediction method.

II. Methodology

A. ATM System based on ADS-B Technique

Based on the ADS-B technique, parameters such as an aerial vehicle's position, heading angle, speed, and identification signal can be automatically obtained from related equipment without manual operation. The ADS-B messages are broadcasted to other aerial vehicles and ground stations. Hence, the air traffic controller (ATC) can better understand the aerial space and monitor the aerial vehicles [14].

The ADS-B sub-system mainly consists of three parts, namely information processing and display, information transmission channel, and information staff [12]. There are three main types of transmission methods for ADS-B messages, which are as follows [27], [28]:

- VHF/UHF digital link mode, whose core technology is the SOTDMA protocol;
- Universal access transceiver, which uses binary continuous phase shift keying system;
- 1090 MHz S-mode extended Squitter, which uses selective interrogation and two-way data communication.

The air traffic management (ATM) can benefit from the ADS-B technique. The ATM generally adopts advanced monitoring, communication, and navigation technologies to dynamically monitor the aerial vehicles' behavior, thereby ensuring that the aerial vehicles can fly in an orderly and safe manner [29]. The ATM system mainly focuses on vertical and horizontal separations among aerial vehicles, and is responsible for guiding, identifying, and monitoring the aerial vehicles. The main components of the ATM system are ground control center, navigation facilities, communication facilities, and radar systems [10].

The ADS-B sub-system can be divided into ADS-B OUT and ADS-B IN modes [30]–[32]. An aerial vehicle equipped with ADS-B computer using onboard navigation receivers can automatically determine its precise position information. The ADS-B transmitter then broadcasts its location information (using the ADS-B OUT mode) every half a second to nearby aerial vehicles and terrestrial ADS-B receivers (i.e., surveillance stations). The ADS-B signal received by other devices is termed as the ADS-B input signal (using the ADS-B IN mode). On the other hand, the signal received by the ground receiver will be transmitted to the ATC, so that the ATC can understand the flight status of an aerial vehicle and to better monitor it. In addition, the ADS-B receivers can be connected to computers and cloud servers, which is promising for researches in the field of AGIVN [33], [34].

B. Aerial Vehicles Conflict Detection

According to ATC regulations, the space around an aerial vehicle is defined as collision avoidance area, and other aerial vehicles are prohibited from entering. Otherwise, there will be the possibility of collision, and collision avoidance measures must be taken [14]. Since it is often impossible to take timely collision avoidance measures in the collision avoidance area, it is necessary to construct an additional protection area to further improve flight safety and collision avoidance flexibility.

In this paper, an additional protection area is constructed outside the collision avoidance area, which is specified by ATC to enhance the collision avoidance performance. Hence, the space around the aerial vehicle is divided into a collision avoidance zone (CAZ) and a protection airspace zone (PAZ) [22], which is shown in Fig. 1. The CAZ is a cylindrical collision avoidance area stipulated by ATC, whose horizontal radius is 9.26 kilometers and the height is 366 meters. Since the ADS-B has a wide working range as large as 185

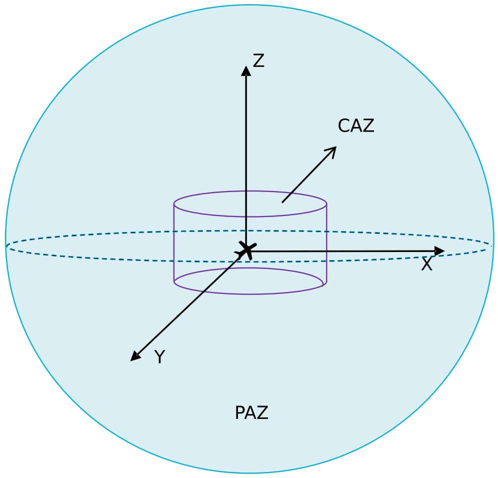

Fig. 1. The space around an aerial vehicle is divided into protection airspace zone and collision avoidance zone.

kilometers of radius, the PAZ is defined as a sphere with a radius of 185 kilometers.

The judgment of route conflict is conducted as follows: when an invading aerial vehicle enters the PAZ of the monitored aerial vehicle, the route conflict detection is triggered. If the invading aerial vehicle route enters the CAZ, it is judged that there is a conflict between the invading aerial vehicle and the target aerial vehicle.

C. Formulation of Aerial Vehicles Conflict Prediction

To execute the conflict detection algorithm, we need to extract the input parameters of the conflict detection algorithm. The work of predicting position and speed information of the aerial vehicles in the future can make the conflict detection and the collision avoidance preparation in advance, which can further improve the safety of the future denser air traffic. Before giving the definition of the input parameters, we first define the position vector **w**, velocity **v**, and velocity vector **s** as follows:

$$\mathbf{w} = [w_1, w_2, w_3] \tag{1}$$

$$\mathbf{v} = [v_1, v_2, v_3] \tag{2}$$

$$\mathbf{s} = [v_g, v_s, \theta] \tag{3}$$

where w_1, w_2, w_3 are the longitude, latitude, and altitude of the aerial vehicles, respectively. v_1, v_2, v_3 are the component velocities of the aerial vehicles on the X-axis, Y-axis and Z-axis, respectively. v_g, v_s, θ are the ground speed, vertical speed, and heading angle of the aerial vehicles, respectively. Hence, the input parameters of the conflict detection algorithm can be defined as the vector **x**, namely:

$$\mathbf{x} = [\mathbf{w}, \mathbf{s}] \tag{4}$$

where **w** and **s** are the position vector and velocity vector of the aircraft at a certain time.

As it is known, artificial intelligence (AI) plays an important role in signal processing, and deep learning is the fastest growing branch of AI [35]–[37]. The deep learning is playing a significant part in many fields such as computer vision, natural language recognition, edge computing, and wireless communications [38]–[42]. Therefore, in this paper, we aim to apply deep learning to conflict prediction algorithm.

The prediction model in this paper can be regarded as a regression model. The data at time t is the input of the neural network, and the predicted data at the next time is the output, which can be formulated as follows:

$$\mathbf{I} = y(x_1, x_2, \cdots, x_t) \tag{5}$$

where x_t is the input vector at time t, y is the function performed by the layers of the neural network, and **I** is the output vector, respectively.

III. Proposed Grouping-Based Conflict Detection Algorithm

A. Acquisition of Wide-Area Surveillance Data

By connecting an ADS-B receiver to a personal computer, ADS-B messages within a specific area can be obtained. The distributed ADS-B surveillance station can work in a cooperative manner to facilitate a wide-area conflict detection. The ADS-B messages mainly contain 6 kinds of information, which can be expressed as:

$$\textbf{message} = [w_1, w_2, w_3, v_g, \theta, v_s] \tag{6}$$

where $w_1, w_2, w_3, v_g, \theta, v_s$ denote the longitude, latitude, altitude, ground speed, heading angle, and vertical speed of the aerial vehicles, respectively.

In order to obtain the required wide-area surveillance dataset, the ADS-B messages can be preprocessed as follows.

Data cleaning: Because the ADS-B messages is obtained by the distributed surveillance stations, and contain flight status information of multiple aerial vehicles at different time, we need to filter the ADS-B messages according to time, and divide the aerial vehicles at different regions and moments into different groups. In addition, we need to remove duplicate data which are introduced by multiple factors [43].

Data conversion: Because the latitude and longitude information contained in the ADS-B messages cannot be used directly in the proposed algorithm, we adopt the World Geodetic System-1984 Coordinate System (WGS-84 coordinate system), and convert the latitude and longitude from the geographic coordinate to the WGS-84, which is written as

$$[X, Y] = f[w_1, w_2] \tag{7}$$

$$Z = w_3 \tag{8}$$

where f is the conversion function from the geographic coordinate to the projected coordinate, and X, Y, Z are the coordinates of the aerial vehicles in the WGS-84 frame. In addition, the proposed algorithm maps the sub-velocities and position coordinates on the X, Y and Z axes to the time axis. Therefore, the ground speed needs to be decomposed:

$$v_x = v_g * cos(\theta) \tag{9}$$

$$v_y = v_g * sin(\theta) \tag{10}$$

$$v_z = v_s \tag{11}$$

where v_x, v_y, v_z are the partial speed of the aerial vehicles on the X, Y, and Z coordinate axes, respectively. After data pre-processing, the ADS-B messages can be standardized.

B. The Idea of Aerial Vehicles Grouping

If two aerial vehicles are far away, the probability of conflict between the two vehicles is very low. Therefore, conflict detection in this scenario is meaningless, and will reduce the efficiency of the algorithm. This problem motivates us to divide the entire space into different regions, and thus the aerial vehicles can be grouped.

First, considering the location of arbitrary two airports P and Q, we construct a rectangular route area as shown in Fig. 2. Then we filter out all the aerial vehicles in the rectangular route area, and build a small rectangle area P1 at the bottom of the large rectangular area, and areas P2, P3, P4 are sequentially built along the boundary of the large rectangle.

Notice that the grouping method will make the next small rectangle overlap with the previous small rectangle. The overlap areas are denoted as Q1, Q2, and Q3 in Fig. 2 (the shaded parts). In this way, the aerial vehicles at the edges of the small rectangles will be detected without omission.

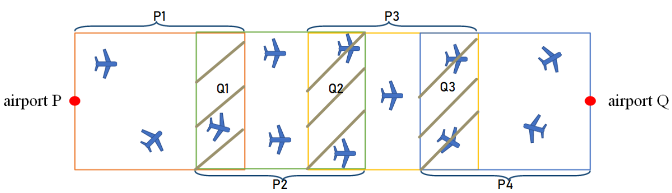

Fig. 2. The overall aerial vehicles are grouped to form several small aerial vehicle groups.

C. Conflict Detection Based on Aerial Vehicles Grouping

We assume that the target aerial vehicle is A and the intruding aerial vehicle is B, and the projected coordinate of A is (X_A, Y_A, Z_A), and the velocity is (V_{xA}, V_{yA}, V_{zA}). The projected coordinate of B is (X_B, Y_B, Z_B), and the velocity is (V_{xB}, V_{yB}, V_{zB}). Assuming a threshold u, the conflict between A and B can be understood as the distance between them is less than u, hence there is a conflict. Specifically, the judgement of the conflict between A and B are based on certain conditions, namely, there exists a certain area in the route that occurs conflicts on the X, Y, and Z axes at the same time [22], which is expressed as

$$|X_A - X_B| < Th_a \tag{12}$$

$$|Y_A - Y_B| < Th_b \tag{13}$$

$$|Z_A - Z_B| < Th_c \tag{14}$$

where X_A, X_B, Y_A, Y_B, Z_A, Z_B represent the distance coordinates (in kilometers) on the X, Y, and Z axes, respectively. Th_a, Th_b, Th_c represent the threshold distance (in kilometers).

By mapping the conflict area on the coordinate axis to the time axis, the above three formulas are converted into conflict time periods $[t_{X1}, t_{X2}], [t_{Y1}, t_{Y2}]$ and $[t_{Z1}, t_{Z2}]$. The existence of a conflict is determined by judging whether there is an intersection between the three conflicting time periods. Since the detection algorithms for the X, Y, and Z axis directions are similar, the X axis is used as an example to illustrate the aerial vehicle route conflict detection algorithm, and the direction of the speed is the positive direction of the X axis.

When $X_A > X_B, V_{xA} > V_{xB}$ or $X_A < X_B, V_{xA} < V_{xB}$, the distance between the two aerial vehicles on the X axis will increase.

When $X_A > X_B, V_{xA} < V_{xB}$ or $X_A < X_B, V_{xA} > V_{xB}$, the distance between the two aerial vehicles on the X axis will decrease.

In general, when $(X_A - X_B)(V_{xA} - V_{xB}) > 0$, the distance between the two aerial vehicles on the X axis will increase; when $(X_A - X_B)(V_{xA} - V_{xB}) < 0$, the distance will decrease. Otherwise, the distance will not change.

The following 5 cases can be obtained [22]:

Case 1: If $(X_A - X_B)(V_{xA} - V_{xB}) \geq 0, |X_A - X_B| \geq Th_a$, it indicates there is no conflict.

Case 2: If $(X_A - X_B)(V_{xA} - V_{xB}) = 0, |X_A - X_B| < Th_a$, it indicates a conflict, and the conflict period is $[t_{X1}, t_{X2}] = [0, +\infty]$.

Case 3: If $(X_A - X_B)(V_{xA} - V_{xB}) > 0, |X_A - X_B| < Th_a$, it indicates a conflict, and the conflict period is $[t_{X1}, t_{X2}] = [0, (Th_a - |X_A - X_B|)/|V_{xA} - V_{xB}|]$.

Case 4: If $(X_A - X_B)(V_{xA} - V_{xB}) < 0, |X_A - X_B| < Th_a$, it indicates a conflict, and the conflict period is $[t_{X1}, t_{X2}] = [0, (Th_a + |X_A - X_B|)/|V_{xA} - V_{xB}|]$.

Case 5: If $(X_A - X_B)(V_{xA} - V_{xB}) < 0, |X_A - X_B| \geq Th_a$, it indicates a conflict, and the conflict period is $[t_{X1}, t_{X2}] = [(Th_a - |X_A - X_B|)/|V_{xA} - V_{xB}|, (Th_a + |X_A - X_B|)/|V_{xA} - V_{xB}|]$.

The above cases show the conflict situations between the two aerial vehicles in the X-axis direction. Similarly, the conflict situations in the Y-axis and Z-axis directions and the conflict time periods can be obtained. The part outside the virtual box in Fig. 3 shows the flowchart of the conflict detection algorithm between two aerial vehicles in the protected area.

If there is a conflict in the protection airspace zone, it is necessary to detect the conflict in the collision avoidance zone [22] which is set as

$$\begin{aligned} Th_a^2 < &\left(\frac{(V_{xA} - V_{xB})(t_1 + t_2)}{2} + X_A - X_B\right)^2 \\ &+ \left(\frac{(V_{yA} - V_{yB})(t_1 + t_2)}{2} + Y_A - Y_B\right)^2 \end{aligned} \tag{15}$$

If the above formula does not hold, it indicates that there is a conflict between the invading aerial vehicle and the target aerial vehicle. Hence, all the conflict cases have been discussed.

IV. Proposed LSTM-Based Conflict Prediction Method

Recurrent neural network (RNN) is one of the most important branches of deep learning [44]–[46]. The RNNs can

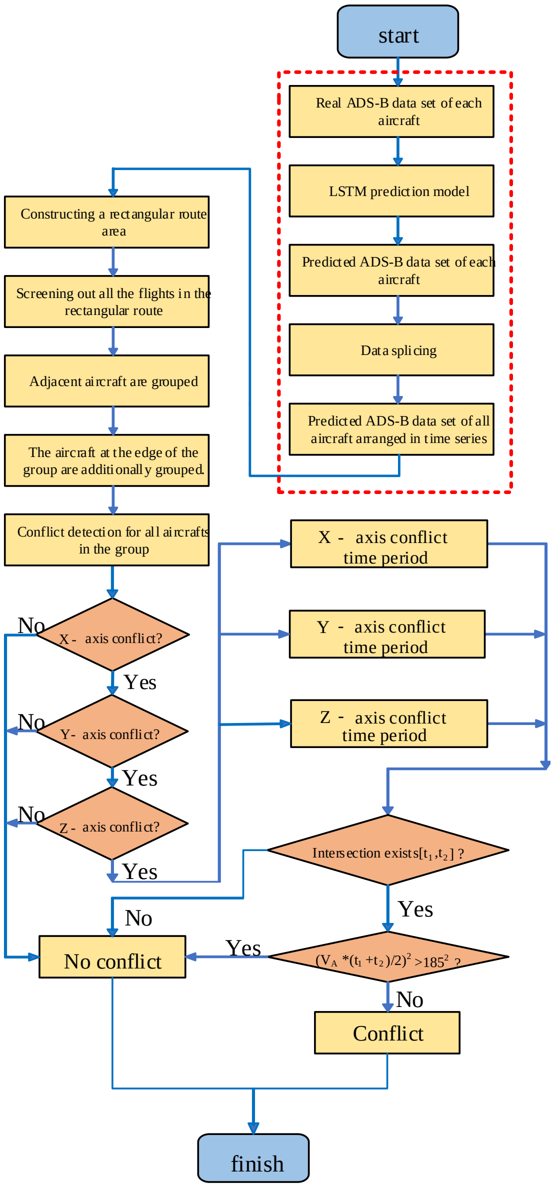

Fig. 3. Flowchart of the proposed conflict prediction algorithm based on trajectory prediction.

deal with sequence processing, and have been widely used in speech recognition, natural language processing, and other fields. The back-propagation through time (BPTT) algorithm is a commonly used method for training the RNNs [45]. The idea is to continuously find a better point along the direction of the negative gradient, and the parameters are updated periodically until convergence.

The problem of gradient disappearance can easily occur when using the BPTT, which is particularly serious when the sequence is relatively long. Therefore, a special case of the RNN, namely LSTM, can be adopted [47]. The LSTM introduces the concept of cell states, and uses three gates named input gate, forget gate, and output gate to maintain and control information passing and parameter update [48], [49]. In this paper, we utilize an architecture that combines the LSTM with fully-connected layers [50], as shown in Fig. 4. In Fig. 4, X and Y represent input and output, respectively, where the subscripts $t, t{+}1, \cdots, t{+}N{-}1$ and $t{+}N, t{+}N{-}1, \cdots, t+2N-1$ represent N times (the sampling interval is 1 second), respectively.

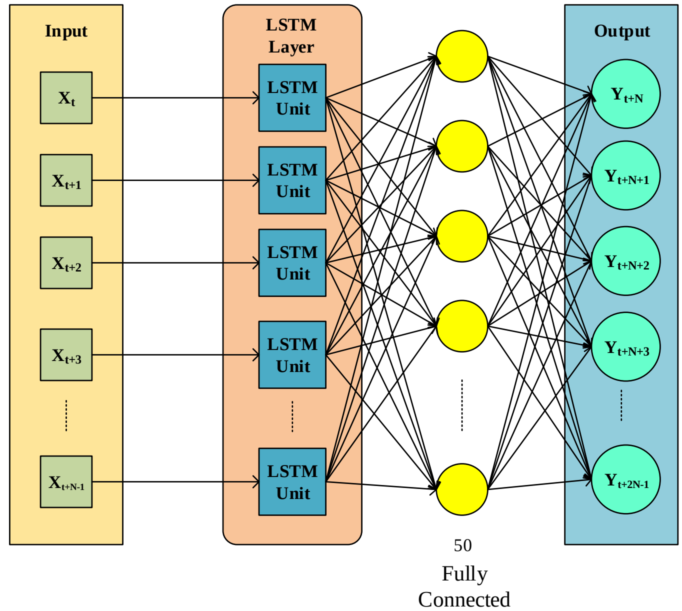

Fig. 4. Trajectory prediction model using LSTM and fully-connected layers.

Algorithm 1 The trajectory prediction algorithm of LSTM-based.

Input: Real ADS-B data sets of aerial vehicles $D = \{d_1, d_2, \ldots, d_N\}$, time step t, lag time τ;
Output: Predicted ADS-B data sets of aerial vehicles $\hat{D}$;

```
Standardize the data sets;
Transform the standardized time series data sets D into the supervised learning data sets D_SL;
for i in 1, 2, 3, ··· , N − t do
    D'_input = {d_i, d_{i+1}, ··· , d_{i+t−1}};
    D'_output = d_{i+t−1+τ};
    A_i = data_splicing(D'_input, D'_output);
end for
D_SL = ensemble(A_1, A_2, ··· , A_{N−t});
Design the LSTM network, then train and test the supervised learning data sets D_SL;
Adjust the network parameters, select the LSTM network with the best performance, and get the corresponding predicted data sets D̂ with the best performance;
return D̂.
```

As explained in Section III, ADS-B messages have been preprocessed to form a dataset, and the input sequences can meet the requirement proposed by the LSTM-based neural network after data cleaning and conversion. The grouped longitude, latitude, altitude, ground speed, vertical speed, and heading angle information of multiple consecutive moments in the dataset are sequentially put into the network for training and testing. Through **Algorithm 1**, we obtain the trajectory information of aerial vehicles at the future time. As a result, the future flight states predicted by the network can be fed into the conflict detection algorithm. Hence, we can predict the conflict situation for the future minutes, and we term the revised algorithm as LSTM-based conflict prediction method. After obtaining the predicted trajectory of each aerial vehicle, we arrange the predicted trajectories in time sequence through data splicing, and finally input the processed dataset into the grouping-based aerial vehicle conflict detection algorithm, as shown in Fig. 3.

V. Proposed CNN-Based Conflict Prediction Method

Convolutional Neural Networks (CNN) is a type of feedforward neural networks that includes convolution calculations and has a deep structure [51]–[53]. In addition, CNN can also perform time series prediction tasks [54]. Hence, a CNN-based method can be also adopted for the trajectory prediction task as a comparison in this paper.

The CNN-based trajectory prediction method is generally similar to the LSTM-based method. The compared structure of the CNN-based method is shown in Fig. 5. The execution process of the compared CNN algorithm is shown in **Algorithm 2**. ADS-B messages of each aerial vehicle can be obtained through the local ADS-B receiver, and the preprocessed and standardized datasets are fed into the CNN network. As shown in Fig.5, the datasets successively go through the convolution operation of the convolutional layer, the maximum pooling of the pooling layer, and the dimensional transformation of the fully-connected layer [55]–[57]. Hence, the predicted trajectories of aerial vehicles can be obtained and finally fed into the grouping-based aerial vehicle conflict detection algorithm.

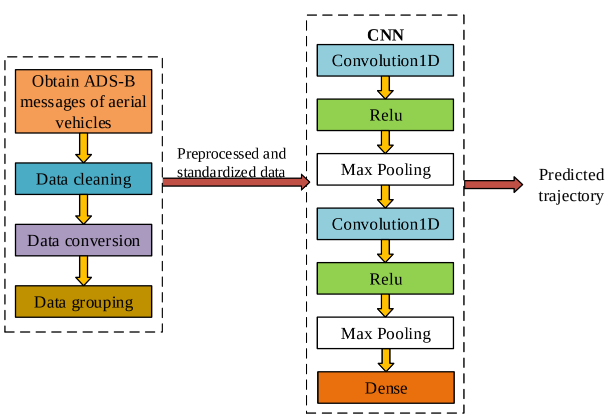

Fig. 5. Structure of the CNN-based network.

VI. Proposed LS-Based Conflict Prediction Method

In a short period, it can be assumed that the trajectory of the aerial vehicles changes linearly, and least square (LS) method is a typical linear regression model. Therefore, this paper also adopts the LS-based method for the trajectory prediction task, which is convenient to make a comparison with the LSTM-based and CNN-based schemes. The principle of the LS-based method is to construct a suitable estimator so that the residual sum of squares (RSS) is minimized [58], as shown below:

$$\left\{\sum_{i=1}^{N} {r_i}^2\right\}_{\min} = \left\{\sum_{i=1}^{N} \left[f(x_i;\alpha_1,\alpha_2,\cdots,\alpha_n) - y_i\right]^2\right\}_{\min} \tag{16}$$

where $\sum_{i=1}^{N} {r_i}^2$ represents RSS, $\alpha_1,\alpha_2,\cdots,\alpha_n$ represent n unknown estimators, $f(x_i;\alpha_1,\alpha_2,\cdots,\alpha_n)$ is the predicted value of $x_1,x_2,\cdots,x_N$ at N different points, and $y_1,y_2,\cdots,y_N$ are the actual values of $x_1,x_2,\cdots,x_N$ at N different points.

Algorithm 2 The trajectory prediction algorithm of CNN-based.

Input: Real ADS-B data sets of aerial vehicles D;
Output: Predicted ADS-B data sets of aerial vehicles $\hat{D}$;
Divide randomly the mixed samples D into training samples and validation samples by $7:3$;
Construct CNN network according to Fig. 5 and choose adaptive moment estimation (Adam) and mean absolute error (MAE) as optimizer and loss function respectively;
Train CNN to minimize loss function;
Adjust the network parameters, select the CNN network with the best performance, and get the corresponding predicted data sets $\hat{D}$ with the best performance;
return $\hat{D}$.

Algorithm 3 The trajectory prediction algorithm of LS-based.

Input: Real ADS-B data sets of aerial vehicles $D = \{d_1,d_2,\cdots,d_N\}$, time step t, lag time τ;
Output: Predicted ADS-B data sets of aerial vehicles $\hat{D}$;
for i in $1,2,3,\ldots,N-t$ **do**
  $data = \{d_i,d_{i+1},\cdots,d_{i+t-1}\}$;
  $time = \{i,i+1,\cdots,i+t-1\}$;
  The curve equation $data = f(time)$ is obtained by data fitting;
  $\hat{data}_{i+t-1+\tau} = f(i+t-1+\tau)$;
end for
$\hat{D} = \text{ensemble}(\hat{data}_{t+\tau},\hat{data}_{t+\tau+1},\cdots,\hat{data}_{N-1+\tau})$;
return $\hat{D}$.

The LS-based method is effective in curve fitting problems. The fitted curve obtained by the LS method can reflect the overall distribution of the data without causing large local fluctuations, and can also reflect the characteristics of the approximated function. The execution process of the proposed LS algorithm is shown in **Algorithm 3**. Unlike the LSTM-based and the CNN-based methods, the LS-based method proposed in this paper executes segmented prediction, namely, it periodically refits a curve with the previous N seconds data to predict the next second data. For example, we use the actual data at time 0 to time t to fit the curve; and according to the fitted curve, we can predict the data at time $t+1$; then we use the actual data at time 1 to time $t+1$ to predict the data at time $t+2$ based on the fitted curve, and so on. Finally, the predicted data are compared with the actual data to analyze the performance.

VII. Experimental Results

In this section, performance of the group-based conflict detection algorithm is evaluated. The trajectory prediction algorithms of LSTM-based, CNN-based and LS-based methods are trained, respectively. Then the three aerial vehicles trajectory prediction models are compared in terms of prediction accuracy. We finally discuss the impact of the trajectory prediction accuracy on the conflict prediction.

A. Results of Route Conflict Detection Algorithm Based on Grouping

In this experiment, since the CAZ is a cylindrical collision avoidance area stipulated by ATC (see Fig. 1), we set its horizontal radius as 9.26 km and its height as 366 meters. Accordingly, we set $Th_a = 9.26$ km, $Th_b = 9.26$ km, $Th_c = 0.366$ km in (12)∼(14). Fig. 6 shows a deployment of the ADS-B-based ground station. The ADS-B omnidirectional antenna is directly connected to the ground monitoring station, and continuously receives ADS-B messages from flight within a diameter of 300 kilometers, which are saved to our computer to facilitate our data processing.

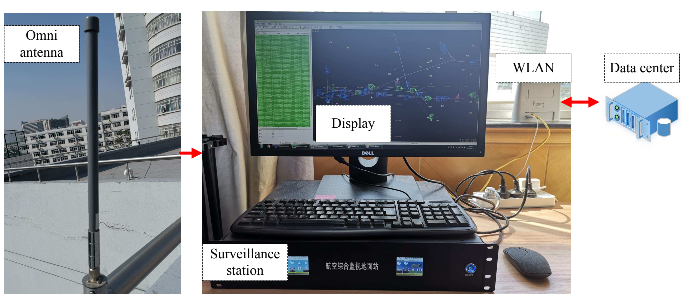

Fig. 6. Deployment of the ADS-B-based ground station.

In this experiment, we adopted our ADS-B platform to obtain all aerial vehicles surveillance information on July 10 of the year 2019. Using the surveillance information, we conducted the conflict detection experiment on 510,000 flight items from 12:00 pm to 1:00 am. Fig. 7 shows the route between Liaocheng and Tangshan at 00:00:10 on July 10. The blue aircrafts represent the conflict-free aerial vehicles. The red aircrafts represent aerial vehicles with conflict warning.

By using the grouping-based conflict detection algorithm, we conducted a conflict detection experiment on the 510,000 items of ADS-B messages from 12:00 pm to 1:00 am. As can be seen from Fig. 7, our experiment based on real-world ADS-B messages can realize the detection and visualization of aerial vehicles conflicts. Since the entire route area is divided into small areas, the burden of calculation can be significantly reduced, and thus the aerial vehicle conflicts can be detected and warned in a real-time manner. Fig. 8 shows the percentage of aerial vehicles conflicts in the total number of aerial vehicles. It is calculated that the average conflict probability in every second is approximately 0.383%.

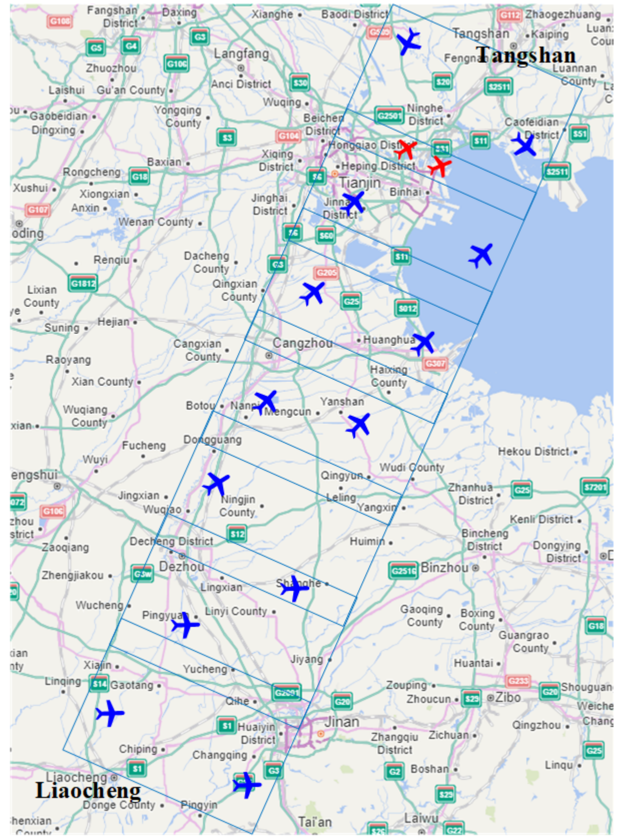

Fig. 7. Visualization of route conflict from Liaocheng city to Tangshan city.

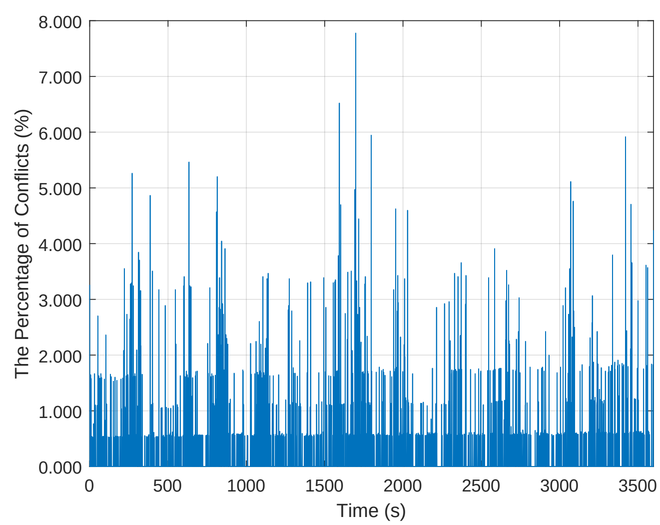

Fig. 8. Aerial vehicle conflicts per second as a percentage of the total number of aerial vehicles.

B. Results of the LSTM-based, CNN-based and LS-based Predictors

Before training the predictor based on the LSTM model, the dataset is divided into multiple datasets according to longitude, latitude, altitude, ground speed, vertical speed, and heading angle. Preprocess of the dataset before training is conducted as follows. Since we use the first n seconds of data to predict the data at t seconds ($t > n$), the data in a period of n seconds and the data after t seconds are bundled into a group. In order to ensure the fairness of the experiment, the input sequences of the CNN-based and the LS-based methods are the same as that of the LSTM-based scheme, including the same length and prediction conditions.

1) Short-term Prediction: In the short-term prediction experiment, we use the flight information of the first 16 seconds to predict the flight information of the next second. First, the items of the dataset are bundled into groups. Then the processed dataset is divided into training set and testing set. Finally, the longitude, latitude, altitude, ground speed, vertical speed, and heading angle data are fed into the LSTM-based model for training and testing, respectively. In this paper, we use root mean squared error (RMSE) to evaluate the prediction performance, which is formulated as follows:

$$RMSE = \sqrt{\frac{1}{N}\sum_{t=1}^{N}(y_t - \hat{y}_t)^2} \tag{17}$$

where N is the total number of samples; y_t is the true values; $\hat{y}_t$ is the predicted values. Results of the LSTM-based, CNN-based and LS-based short-term prediction are depicted in Fig. 9. The light blue line, green line, and red line represent the predicted values of the LS-based, CNN-based, and LSTM-based methods, respectively. The dark blue line represents the true values.

2) Long-term Prediction: Because the LSTM units are good at dealing with long-term memory, we evaluate the performance of the LSTM-based scheme in terms of making long-term prediction [47]. In this experiment, the flight information of the aerial vehicles in a period of 16 seconds (e.g., from the 10^{th} second to the 25^{th} second) is used to predict the flight information after 40 seconds (e.g., the 65^{th} second). We term this task as mid-term prediction. In addition, in order to enable the conflict alert can be triggered several minutes in advance, we evaluate minute-level trajectory predictions of aerial vehicles. In this section, the flight information of aerial vehicles in a period of 60 seconds (e.g., from the 1^{st} second to the 60^{th} second) is used to predict the flight information after 60 seconds (e.g., the 120^{th} second). We term this task as long-term prediction. Experiments are also conducted by the CNN-based and LS-based methods. Results of the LSTM-based, CNN-based and LS-based mid-term predictions are shown in Fig. 10. And results of the long-term prediction are shown in Fig. 11.

3) Analysis: RMSE scores of the three different predictors are listed in Table I. It can be seen that the deep-learning-based prediction models (i.e., LSTM, CNN) show better prediction performance than the utilized traditional machine learning model (i.e., LS). Specifically, the scores of the LSTM-based predictor are generally smaller than the CNN-based and LS-based predictors. However, in order to reach convergence point, the LSTM-based model requires more training time (6,000 iterations), while the CNN-based model requires 1,000 iterations and the LS-based model only takes a few seconds. It can be concluded that the LSTM-based predictor obtains better accuracy at the expense of adequate training.

In detail, the short-term prediction experiment shows that the LSTM-based, CNN-based and LS-based methods can predict the trajectories of the aerial vehicles with relatively low errors. The RMSE scores for the six metrics have differences, however, the prediction performance of LSTM-based is the best of the three methods. On the other hand, compared with the short-term prediction, the mid-term prediction experiment shows that the prediction errors increased. In addition, in terms of the long-term prediction tasks, when selected prediction time steps increase (from 40 seconds to 60 seconds), the three prediction models (especially the LSTM-based model) make their prediction errors generally lower than the mid-term prediction tasks by increasing the length of their input sequences (from 16 seconds to 60 seconds). Meanwhile, the prediction errors of the CNN-based and LS-based methods are much larger than that of the LSTM-based model, which demonstrates the effectiveness of LSTM units when dealing with the long-term prediction tasks.

C. Conflict detection of aerial vehicles based on trajectory prediction

In this section, we use LSTM to conduct conflict detection experiments on the predicted values of aerial vehicles trajectories. The datasets we use here are also the ADS-B data we collected from 12:00 pm to 1:00 am on July 10, 2019. We used the trajectory information of each aerial vehicle every 16 seconds to predict the trajectory information of the next second. Finally, the predicted aerial vehicle trajectory information from 12:00 pm to 1:00 am formed approximately 500,000 items. Using the proposed grouping-based conflict detection algorithm, we conducted conflict detection experiments on the 500,000 items. The experimental results are as depicted in Fig. 12∼13.

Fig. 12 shows the percentage of conflicting aerial vehicles in the total number of aerial vehicles. The calculation results show that by using the trajectory prediction method, the average probability of detected conflicts per second is about 0.290%. Fig. 13 compares the difference between the number of detected conflicts and the number of predicted conflicts. Compared with the average conflict probability of 0.383% obtained by using the actual trajectories, the average conflict probability based on the predicted trajectories is slightly lower. It is inferred that the predicted trajectories could be more ideal, while the real trajectories have sudden variations. We also calculated the RMSE score for evaluating the defect when using the predicted trajectories, and the RMSE score was 0.8610. In fact, there could be an error in the trajectory information obtained from ADS-B receiver, but the error can be usually about 100 meters [24], which has little impact on the trajectory prediction tasks. If transmission process of

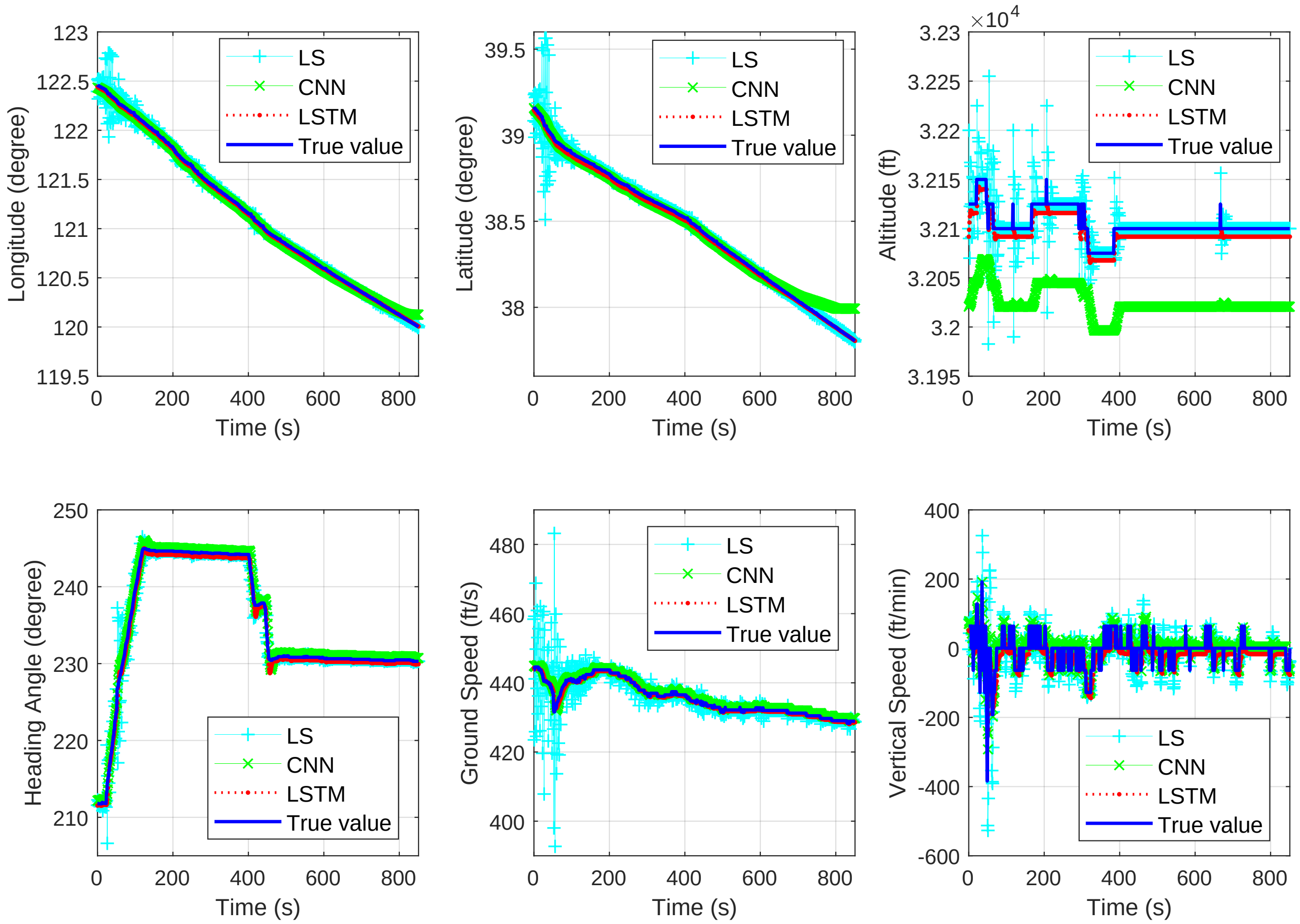

Fig. 9. Predicted short-term trajectories by using the LSTM-based, CNN-based and LS-based predictors.

TABLE I
PERFORMANCE COMPARISON OF THE LSTM-BASED, CNN-BASED AND LS-BASED SHORT-TERM, MID-TERM, LONG-TERM PREDICTION TASKS

	The LSTM-based short-term prediction error	**The LSTM-based mid-term prediction error**	**The LSTM-based long-term prediction error**	**The CNN-based short-term prediction error**	**The CNN-based mid-term prediction error**	**The CNN-based long-term prediction error**	**The LS-based short-term prediction error**	**The LS-based mid-term prediction error**	**The LS-based long-term prediction error**
Longitude (degree)	0.011	0.02	0.028	0.0247	0.045	0.076	0.054	0.339	0.286
Latitude (degree)	0.013	0.073	0.031	0.0468	0.078	0.126	0.058	0.468	0.408
Altitude (ft)	9.338	66.273	28.626	79.6723	32.526	138.706	17.357	718.344	665.836
Ground Speed (ft/s)	0.529	2.582	2.572	0.9058	2.979	2.797	4.511	4.732	4.747
Vertical Speed (ft/min)	39.515	45.329	44.850	37.1091	55.249	45.453	52.028	201.841	111.822
Heading Angle (degree)	0.491	4.704	6.295	0.6037	5.025	6.596	1.076	4.710	7.552

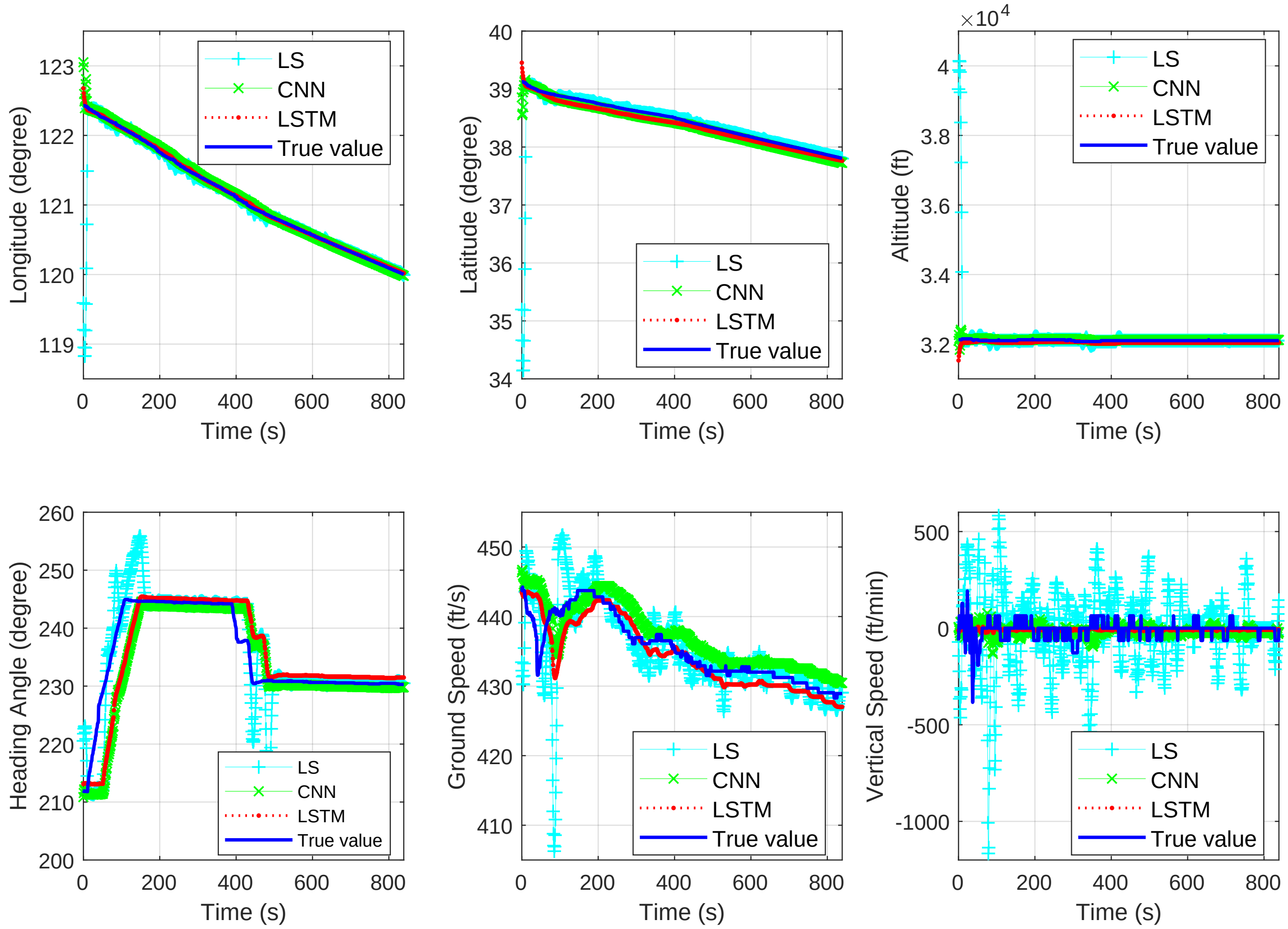

Fig. 10. Predicted mid-term trajectories by using the LSTM-based, CNN-based and LS-based predictors.

the error is further considered, the RMSE score calculated by the conflict detection method based on the trajectory prediction could be increased from 0.8610 to about 1 at most, which is still within the error range allowed by the conflict detection method. The result means that the predicted number of conflicts per second differs from the actual number by less than one aerial vehicle. Hence, the proposed method makes it is possible to detect whether there would be conflicts in the future seconds.

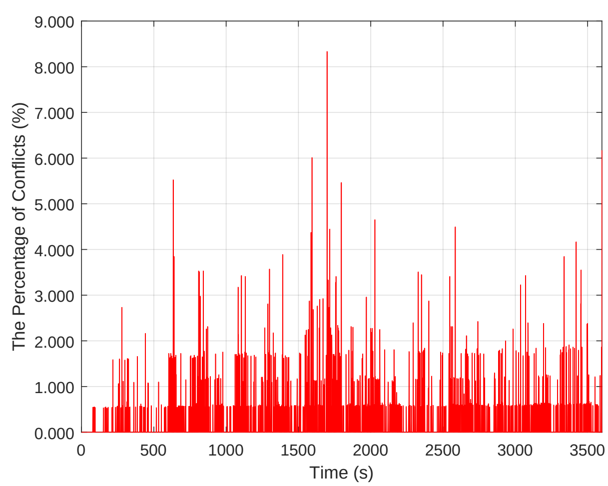

Fig. 12. Predicted aerial vehicle conflicts per second as a percentage of the total number of aerial vehicles based on trajectory prediction.

VIII. Conclusion

This paper proposes a conflict detection algorithm based on an aerial vehicles grouping strategy. In order to further improve the timeliness of conflict detection, we use the LSTM-based, the CNN-based and the LS-based methods to predict the trajectory of aerial vehicles, respectively. The trajectory prediction experiments are divided into short-term, mid-term, and long-term predictions. The results show that the short-term predictions can be more accurate than the mid-term and long-term predictions. In addition, the LSTM-based model generally outperforms the CNN-based and the LS-based methods in three prediction tasks, especially when predicting the mid-term and long-term trajectory of aerial vehicles. However, the problem is that for the mid-term and long-term predictions, the performance degradation will affect the performance of the conflict detection algorithm. Therefore, in order to overcome this problem, our future work will focus on designing more reliable neural networks and integrating more effective information into the training dataset. Finally, we evaluate influence of the trajectory prediction on the conflict detection algorithm. The experimental results

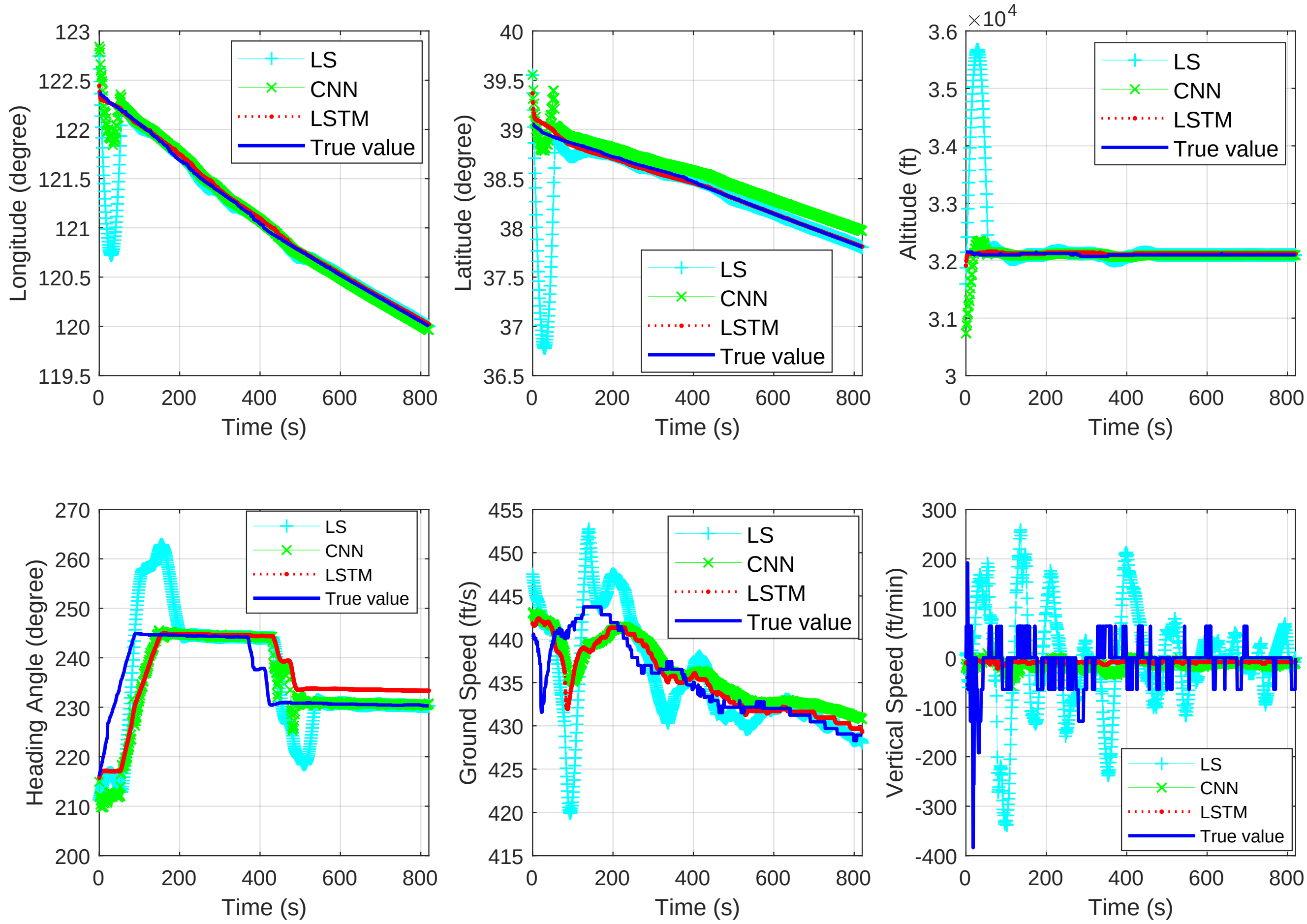

Fig. 11. Predicted long-term trajectories by using the LSTM-based, CNN-based and LS-based predictors.

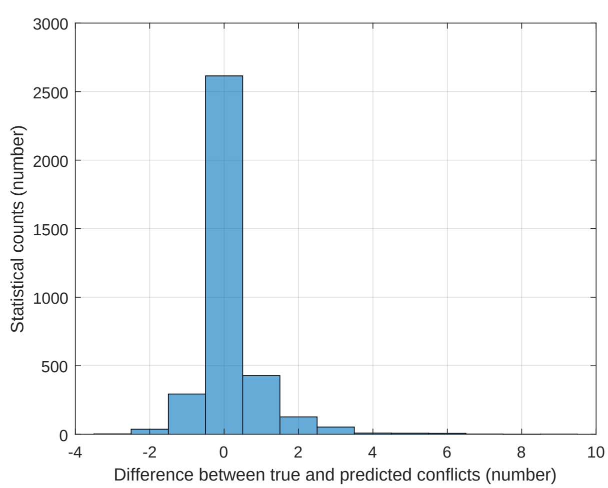

Fig. 13. Statistical difference between the actual number of conflicts and the predicted number of conflicts, and the RMSE score is 0.8610.

demonstrate the effectiveness of integrating the grouping strategy, the trajectory detection based on machine learning, and the conflict detection.

REFERENCES

[1] J. Sun, F. Liu, Y. Zhou, G. Gui, T. Ohtsuki, S. Guo, and F. Adachi, "Surveillance plane aided air-ground integrated vehicular networks: architectures, applications, and potential," *IEEE Wireless Communications*, vol. 27, no. 6, pp. 122–128, Dec. 2020.

[2] S. Zhang, W. Quan, J. Li, W. Shi, P. Yang and X. Shen, "Air-ground integrated vehicular network slicing with content pushing and caching," *IEEE Journal on Selected Areas in Communications*, vol. 36, no. 9, pp. 2114–2127, Sept. 2018.

[3] J. Sun, G. Gui, H. Sari, H. Gacanin, F. Adachi, "Future air-ground vehicle networks: challenges and opportunities," *IEEE Vehicular Technology Magazine*, to appear, doi: 10.1109/MVT.2020.3014598, 2020.

[4] J. Liu, Y. Shi, Z. Md. Fadlullah, and N. Kato, "Space-air-ground integrated network: a survey," *IEEE Communications Surveys & Tutorials*, vol. 20, no. 4, pp. 2714–2741, 2018.

[5] C. Mishra, S. Maskell, S. Au and J. F. Ralph, "Efficient estimation of probability of conflict between air traffic using subset simulation," *IEEE Transactions on Aerospace and Electronic Systems*, vol. 55, no. 6, pp. 2719–2742, Dec. 2019.

[6] J. Naganawa, J. Honda, T. Otsuyama, H. Tajima and H. Miyazaki, "Evaluating path loss by extended squitter signals for aeronautical surveillance," *IEEE Antennas and Wireless Propagation Letters*, vol. 16, pp. 1353–1356, May 2017.

[7] S. Neemat and M. Inggs, "Design and implementation of a digital realtime target emulator for secondary surveillance radar/identification friend or foe," *IEEE Aerospace and Electronic Systems Magazine*, vol. 27, no. 6, pp. 17–24, Jun. 2012.

[8] N. Petrochilos and A. van der Veen, "Algebraic algorithms to separate overlapping secondary surveillance radar replies," *IEEE Transactions on Signal Processing*, vol. 55, no. 7, pp. 3746–3759, Jul. 2007.

[9] J. A. F. Zuluaga, J. F. V. Bonilla, J. D. O. Pabon, and C. M. S. Rios, "Radar error calculation and correction system based on ads-b and business intelligent tools," *Proc. Int. Carnahan Conf. Secur. Technol.*, pp. 1–5, IEEE, 2018.

[10] Y. Zhou, Y. Wan, S. Roy, C. Taylor, C. Wanke, D. Ramamurthy, and J. Xie, "Multivariate probabilistic collocation method for effective uncertainty evaluation with application to air traffic flow management," *IEEE Transactions on Systems, Man, and Cybernetics: Systems*, vol. 44, no. 10, pp. 1347–1363, Oct. 2014.

[11] A. Yang, X. Tan, J. Baek, and D. S. Wong, "A new ADS-B authentication framework based on efficient hierarchical identity-based signature with batch verification," *IEEE Transactions on Services Computing*, vol. 10, no. 2, pp. 165–175, Mar-Apr 2017.

[12] S. Jheng, S. Jan, Y. Chen and S. Lo, "1090 MHz ADS-B-based wide area multilateration system for alternative positioning navigation and timing," *IEEE Sensors Journal*, vol. 20, no. 16, pp. 9490–9501, Aug. 2020.

[13] Y. A. Nijsure, G. Kaddoum, G. Gagnon, F. Gagnon, C. Yuen, and R. Mahapatra, "Adaptive air-to-ground secure communication system based on ADS-B and wide-area multilateration," *IEEE Transactions on Vehicular Technology*, vol. 65, no. 5, pp. 3150–3165, 2015.

[14] M. Strohmeier, M. Schafer, V. Lenders, and I. Martinovic, "Realities and challenges of nextgen air traffic management: The case of ABS-B," *IEEE Communications Magazine*, vol. 52, no. 5, pp. 111–118, May 2014.

[15] X. Sun, Y. Li, N. Wang, Z. Li, M. Liu, and G. Gui, "Towards selfadaptive selection of kernel functions for support vector regression in IoT based marine data prediction," *IEEE Internet Things of Journal*, to appear, doi: 10.1109/JIOT.2020.2988050.

[16] M. Mohamed and A. Allam, "Design and implementation of a directional antenna for a traffic alert and collision avoidance system (TCAS)," *18th Mediterranean Microwave Symposium (MMS)*, Istanbul, pp. 79–82, 2018.

[17] X. Tang, J. Xing and S. Han, "Runway incursion prevention method based on a discrete object sensing event-driven model," *IET Intelligent Transport Systems*, vol. 8, no. 6, pp. 558–569, Sept. 2014.

[18] D. De and P. K. Sahu, "Design of an endfire microstrip antenna for aircraft collision avoidance system," *IEEE Antennas and Wireless Propagation Letters*, vol. 18, no. 5, pp. 996–1000, May 2019.

[19] A. R. Pritchett, R. A. Haga and H. Li, "Attempting to automate compliance to aircraft collision avoidance advisories," in *IEEE Transactions on Automation Science and Engineering*, vol. 13, no. 1, pp. 18–25, Jan. 2016.

[20] G. Xiao, Y. Xu, C. Dai, Z. Jing and J. Wu, "A selection algorithm for conflict aircrafts and performance analysis based on ADS-B," *IEEE/AIAA 30th Digital Avionics Systems Conference, Seattle, WA*, pp. 1–6, 2011.

[21] B. Zhou, H. J. Wang, et al, "A preprocessing method for conflict detection based on ADS-B IN", *Electro-optic and Control*, vol. 24, no. 10, pp. 64–68, Oct. 2017.

[22] B. Li, S. Y. Zhai, R. Li, "ADS-B-based time-axis mapping route conflict detection algorithm", *Electro-optic and Control*, vol. 26, no. 03, pp. 12–15, Mar. 2019.

[23] M. Leonardi, "ADS-B anomalies and intrusions detection by sensor clocks tracking," *IEEE Trans. Aerosp. Electron. Syst.*, to be published, doi: 10.1109/TAES.2018.2886616.

[24] X. Shen, P. Tang, S. Zhang, and W. Jiao, "Quality analysis of navigation uncertain category for position based on ADS-B statistical data," *Acta Aeronautica et Astronautica Sinica*, vol. 36, no. 09, pp. 3128–3136, Sept. 2015.

[25] Z. Shi, M. Xu, Q. Pan, B. Yan, and H. Zhang, "LSTM-based flight trajectory prediction," *International Joint Conference on Neural Networks (IJCNN)*, pp. 1–8, IEEE, 2018.

[26] H. Palangi, L. Deng, Y. Shen, J. Gao, X. He, J. Chen, X. Song, and R. Ward, "Deep sentence embedding using long short-term memory networks: Analysis and application to information retrieval," *IEEE/ACM Transactions on Audio, Speech, and Language Processing*, vol. 24, no. 4, pp. 694–707, Apr. 2016.

[27] Z. Wu, A. Guo, M. Yue and L. Liu, "An ADS-B message authentication method based on certificateless short signature," *IEEE Transactions on Aerospace and Electronic Systems*, vol. 56, no. 3, pp. 1742–1753, Jun. 2020.

[28] J. Sun, J. Ellerbroek and J. M. Hoekstra, "pyModeS: Decoding mode-S surveillance data for open air transportation research," *IEEE Transactions on Intelligent Transportation Systems*, vol. 21, no. 7, pp. 2777–2786, July 2020.

[29] M. Strohmeier, M. Schafer, V. Lenders and I. Martinovic, "Realities and challenges of nextgen air traffic management: The case of ABS-B," *IEEE Communications Magazine*, vol. 52, no. 5, pp. 111–118, May 2014.

[30] D. He, N. Kumar, K.-K. R. Choo and W. Wu, "Efficient hierarchical identity-based signature with batch verification for automatic dependent surveillance-broadcast system," *IEEE Transactions on Information Forensics and Security*, vol. 12, no. 2, pp. 454–464, Feb. 2017.

[31] R. Holdsworth, J. Lambert, and N. Harle, "Inflight path planning replacing pure collision avoidance, using ADS-B," *IEEE Transactions on IEEE Aerospace and Electronic Systems*, vol. 16, no. 2, pp. 27–32, Feb. 2001.

[32] D. He, N. Kumar, K.-K. R. Choo, and W. Wu, "Efficient hierarchical identity-based signature with batch verification for automatic dependent surveillance-broadcast system," *IEEE Trans. Inf. Forensics Secur.*, vol. 12, no. 2, pp. 454–464, Feb. 2017.

[33] Y. A. Nijsure, G. Kaddoum, G. Gagnon, F. Gagnon, C. Yuen and R. Mahapatra, "Adaptive air-to-ground secure communication system based on ADS-B and wide-area multilateration," *IEEE Transactions on Vehicular Technology*, vol. 65, no. 5, pp. 3150–3165, May 2016.

[34] M. Liu, G. Gui, N. Zhao, J. Sun, G. Haris, and H. Sari, "UAV-aided air-to-ground cooperative non-orthogonal multiple access," *IEEE Internet of Things Journal*, vol. 7, no. 4, pp. 2704–2715, Apr. 2020.

[35] Y. Wang, J. Wang, W. Zhang, J. Yang and G. Gui, "Deep learning-based cooperative automatic modulation classification method for MIMO systems," *IEEE Transactions on Vehicular Technology*, vol. 69, no. 4, pp. 4575–4579, Apr. 2020.

[36] Y. Wang, L. Guo, Y. Zhao, J. Yang, B. Adebisi, H. Gacanin, and G. Gui, "Distributed learning for automatic modulation classification in edge devices," *IEEE Wireless Commu. Lett.*, vol. 9, no. 12, pp. 2177–2181, Dec. 2020.

[37] Y. Lin, Y. Tu, Z. Dou, L. Chen, and S. Mao, "Contour stella image and deep learning for signal recognition in the physical layer," *IEEE Transactions on Cognitive Communications and Networking*, early access, doi: 10.1109/TCCN.2020.3024610.

[38] J. Sun, J. Wang, L. Guo, J. Yang and G. Gui, "Adaptive deep learning aided digital predistorter considering dynamic envelope," *IEEE Transactions on Vehicular Technology*, vol. 69, no. 4, pp. 4487–4491, Apr. 2020.

[39] T. Yang, H. Feng, C. Yang, Y. Wang, J. Dong, and M. Xia, "Multivessel computation offloading in maritime mobile edge computing network," *IEEE Internet of Things Journal*, vol. 6, no. 3, pp. 4063–4073, June 2019.

[40] K. Zhang, Y. Zhu, S. Maharjan, and Y. Zhang, "Edge intelligence and blockchain empowered 5G beyond for industrial internet of things," *IEEE Network Magazine*, vol. 33, no. 5, pp.12–19, Sep/Oct. 2019.

[41] G. Gui, M. Liu, F. Tang, N. Kato, and F. Adachi, "6G: Opening new horizons for integration of comfort, security and intelligence," *IEEE Wireless Commun. Mag.*, vol. 27, no. 5, pp. 126–132, Oct. 2020.

[42] Z. Zhang, Y. Li, C. W. Huang, Q. Guo, C. Yuen, and Y. L. Guan, "DNN-aided block sparse Bayesian learning for user activity detection and channel estimation in grant-free non-orthogonal random access," *IEEE Transactions on Vehicular Technology*, vol. 68, no. 12, pp. 12000–12012, Dec. 2019.

[43] G. Gui, F. Liu, J. Sun, J. Yang, Z. Zhou and D. Zhao, "Flight delay prediction based on aviation big data and machine learning," *IEEE Transactions on Vehicular Technology*, vol. 69, no. 1, pp. 140–150, Jan. 2020.

[44] L. Jin, S. Li, and B. Hu, "RNN models for dynamic matrix inversion: A control-theoretical perspective," *IEEE Transactions on Industrial Informatics*, vol. 14, no. 1, pp. 189–199, Jan. 2017.

[45] H. Huang, Y. Peng, J. Yang, W. Xia, and G. Gui, "Fast beamforming design via deep learning," *IEEE Transactions on Vehicular Technology*, vol. 69, no. 1, pp. 1065–1069, Jan. 2020.

[46] R. Chandra, "Competition and collaboration in cooperative coevolution of elman recurrent neural networks for time-series prediction," *IEEE Transactions on Neural Networks and Learning Systems*, vol. 26, no. 12, pp. 3123–3136, Dec. 2015.

[47] Y. Hu, X. Sun, X. Nie, Y. Li, and L. Liu, "An enhanced LSTM for trend following of time series," *IEEE Access*, vol. 7, no. 1, pp. 34020–34030, 2019.

[48] Z. Ma, J. Xing, M. Mesbah, and L. Ferreira, "Predicting short-term bus passenger demand using a pattern hybrid approach," *Transportation Research Part C: Emerging Technologies*, vol. 39, no. 2, pp. 148–163, 2014.

[49] X. Jiang, L. Zhang, and X. M. Chen, "Short-term forecasting of high-speed rail demand: A hybrid approach combining ensemble empirical

mode decomposition and gray support vector machine with real-world applications in china," *Transportation Research Part C: Emerging Technologies*, vol. 44, no. 7, pp. 110–127, 2014.

[50] G. Gui, Z. Zhou, J. Wang, F. Liu and J. Sun, "Machine learning aided air traffic flow analysis based on aviation big data," *IEEE Transactions on Vehicular Technology*, vol. 69, no. 5, pp. 4817–4826, May 2020.

[51] H. Liang, X. Zhang, J. Zhang, Q. Li, S. Zhou, and L. Zhao, "A novel adaptive resource allocation model based on SMDP and reinforcement learning algorithm in vehicular cloud system," *IEEE Transactions on Vehicular Technology*, vol. 68, no. 10, pp. 10018–10029, Oct. 2019.

[52] J. Zhang, X. Tao, H. Wu, N. Zhang, and X. Zhang, "Deep reinforcement learning for throughput improvement of uplink grant-free NOMA system," *IEEE Internet of Things Journal*, vol. 7, no. 7, pp. 6369–6379, Jul. 2020.

[53] Z. Shi, W. Gao, S. Zhang, J. Liu, N. Kato, "AI-enhanced cooperative spectrum sensing for non-orthogonal multiple access," *IEEE Wireless Communications Magazine*, in press, doi: 10.1109/MNET.001.1900305.

[54] L. Ma and S. Tian, "A hybrid CNN-LSTM model for aircraft 4D trajectory prediction," *IEEE Access*, vol. 8, pp. 134668–134680, Jul. 2020.

[55] K. Zhang, Y. Zhu, S. Leng, Y. He, S. Maharjan and Y. Zhang, "Deep learning empowered task offloading for mobile edge computing in urban informatics," *IEEE Internet of Things Journal*, vol. 6, no. 5, pp. 7635–7647, Oct. 2019.

[56] K. Zhang, S. Leng, X. Peng, P. Li, S. Maharjan, and Y. Zhang, "Artificial intelligence inspired transmission scheduling in cognitive vehicular communications and networks," *IEEE Internet of Things Journal*, vol. 6, no. 2, pp. 1987–1997, Apr. 2019.

[57] T. Yang, H. Feng, "Two-stage offloading optimization for energy-latency tradeoff with mobile edge computing in maritime networks," *IEEE Internet of Things Journal*, vol. 7, no. 7, pp. 5954–5963, Jul. 2020.

[58] F. Harrou, Y. Sun, M. Madakyaru and B. Bouyedou, "An improved multivariate chart using partial least squares with continuous ranked probability score," *IEEE Sensors Journal*, vol. 18, no. 16, pp. 6715–6726, Aug. 2018.

Cheng Cheng received the B.S. degree from the Nanjing University of Posts and Telecommunications, Nanjing, China, in 2019. Since 2019, he is currently pursuing the master's degree in communication and information engineering with the Nanjing University of Posts and Telecommunications, Nanjing, China. His research interest includes machine learning for wireless communications.

Liang Guo is now Deputy Director of Data Center Research Department, Institute of Cloud Computing and Big Data, China Academy of Information and Communications Technology. He is a Senior Engineer, Co-Chairman of the Ad Hoc Group of Industrial Data Center of Industrial Internet Industry Alliance, and Head of the Working Group on New Technologies and Testing of Open Data Center Committee. He has been engaged in policy support, technical research and standard-setting in data center, network and IT.

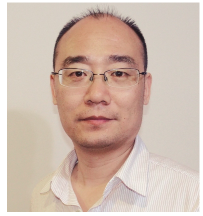

Tong Wu is currently an associate researcher and deputy director with the radio Department of Chinese Academy of Metrology, EMC certification center, bioenergy and Environment Research Institute, new energy and Environment Research Institute and information and Electronics Institute. He served as the Secretary of the National Technical Working Group for standardization of assessment methods in the fields of electricity, magnetism and electromagnetism.

Jinlong Sun (Member, IEEE) received the M.S. and Ph.D. degrees from the Harbin Institute of Technology, Harbin, China, in 2014 and 2018, respectively. He is currently working as an assistant professor with Nanjing University of Posts and Telecommunications, Nanjing, China. His current research interests include signal processing for wireless communications, machine learning, and integrated navigation systems.

Guan Gui (Senior Member, IEEE) received the Ph.D. degree from the University of Electronic Science and Technology of China, Chengdu, China, in 2012. From 2009 to 2014, he joined the Tohoku University as a research assistant as well as a postdoctoral research fellow, respectively. From 2014 to 2015, he was an Assistant Professor in the Akita Prefectural University. Since 2015, he has been a professor with Nanjing University of Posts and Telecommunications, Nanjing, China. His recent research interests include artificial intelligence, deep learning, non-orthogonal multiple access, intelligent semantic communications, and physical layer security.

He is an IEEE Senior Member. Dr. Gui has published more than 200 IEEE Journal/Conference papers and won several best paper awards, e.g., ICC 2017, ICC 2014 and VTC 2014-Spring. He received the Member and Global Activities Contributions Award in 2018, the Top Editor Award of IEEE TRANSACTIONS ON VEHICULAR TECHNOLOGY in 2019, the Outstanding Journal Service Award of KSII TRANSACTIONS ON INTERNET AND INFORMATION SYSTEM in 2020, the Exemplary Reviewer Award of IEEE COMMUNICATIONS LETTERS in 2017. He was also selected as for the Jiangsu Specially-Appointed Professor in 2016, the Jiangsu High-level Innovation and Entrepreneurial Talent in 2016, the Jiangsu Six Top Talent in 2018, the Nanjing Youth Award in 2018. He is serving or served on the editorial boards of several journals, including IEEE TRANSACTIONS ON VEHICULAR TECHNOLOGY, IEICE Transactions on Communications, Physical Communication, Wireless Networks, IEEE ACCESS, Security and Communication Networks, IEICE Communications Express, and KSII Transactions on Internet and Information Systems, Journal on Communications. In addition, he served as Vice-Chair of IEEE WCNC 2021, TPC Chair of IEEE PHM 2021, General Co-Chair of Mobimedia 2020, TPC Chair of WiMob 2020, Track Chairs of IEEE VTC 2020 spring, ISNCC 2020 and ICCC 2020, Award Chair of IEEE PIMRC 2019, and TPC member of many IEEE international conferences, including GLOBECOM, ICC, WCNC, PIRMC, VTC, and SPAWC.

Bamidele Adebisi received his Bachelor's degree in electrical engineering from Ahmadu Bello University, Zaria, Nigeria, in 1999, and his Master's degree in advanced mobile communication engineering and Ph.D. degree in communication systems from Lancaster University, United Kingdom, in 2003 and 2009, respectively. He was a senior research associate with the School of Computing and Communication, Lancaster University, from 2005 to 2012. He joined Manchester Metropolitan University in 2012, where he is currently a reader in electrical and electronic engineering. He has worked on several commercial and government projects focusing on various aspects of wireline and wireless communications. He is particularly interested in research and development of communication technologies for electrical energy monitoring/management, transport, water, critical infrastructures protection, home automation, IoT, and cyber physical systems. He has several publications and a patent in the research area of data communications over power line networks and smart grid. He is a member of IET.

Haris Gacanin (Fellow, IEEE) received the Dipl.-Ing. degree in electrical engineering from the University of Sarajevo, in 2000, and the M.Sc. and Ph.D. degrees from Tohoku University, Japan, in 2005 and 2008, respectively. He was a Japan Society for Promotion of Science Postdoctoral Fellow and an Assistant Professor with Tohoku University, from 2008 to 2010. In 2010, he joined Alcatel-Lucent (now Nokia), where he led the research department at Nokia Bell Labs. He is currently a Full (Chair) Professor with RWTH Aachen University, Germany. His professional interests include the broad area of digital signal processing and artificial intelligence with applications in communication systems. He has more than 200 scientific publications (journals, conferences, and patent applications) and invited/tutorial talks. He is an IEEE VTS Distinguished Lecturer, and he acted as the general chair and a technical program committee member of various international conferences. He was a recipient of several Nokias awards for innovations, the IEICE Communication System Study Group (2015) Award, the 2013 Alcatel-Lucent Award of Excellence, the 2012 KDDI Foundation Research Award, the 2009 KDDI Foundation Research Grant Award, the 2008 Japan Society for Promotion of Science (JSPS) Postdoctoral Fellowships for Foreign Researchers, the 2005 Active Research Award in Radio Communications, the 2005 Vehicular Technology Conference (VTC 2005-Fall) Student Paper Award from the IEEE VTS Japan Chapter, and the 2004 Institute of IEICE Society Young Researcher Award. He is an Associate Editor of IEEE Communications Magazine and previously, serviced at IEICE Transactions on Communications and IET Communications.

Hikmet Sari (Life Fellow, IEEE) received the engineering diploma and the Ph.D. degree from ENST, Paris, France, and the Habilitation degree from the University of Paris XI.,From 1980 to 2002, he held various research and management positions at Philips Research Laboratories, SAT, Alcatel, Pacific Broadband Communications, and Juniper Networks. From 2003 to 2016, he was a Professor and the Head of the Telecommunications Department, Suplec, and a Chief Scientist at Sequans Communications. He is currently a Professor with the Nanjing University of Posts and Telecommunications (NJUPT). Dr. Sari's distinctions include the Andre Blondel Medal in 1995, the Edwin H. Armstrong Achievement Award in 2003, the Harold Sobol Award in 2012, as well as election to the Academia Europaea (Academy of Europe) and the Science Academy of Turkey in 2012. He was the Chair of the Communication Theory Symposium of ICC 2002, a Technical Program Chair of ICC 2004, a Vice General Chair of ICC 2006, a General Chair of PIMRC 2010, a General Chair of WCNC 2012, an Executive Chair of WCNC 2014, a General Chair of ICUWB 2014, a General Co-Chair of IEEE BlackSeaCom 2015, a Technical Program Chair of EuCNC 2015, an Executive Co-Chair of ICC 2016, a General Co-Chair of ATC 2016, an Executive Chair of ICC 2017, a General Co-Chair of ATC 2018, and a General Co-Chair of PIMRC 2019. He also chaired the Globecom and ICC Technical Content (GITC) Committee from 2010 to 2011, and was the Communications Society (ComSoc) Vice President for Conferences from 2014 to 2015, the Director for Conference Operations of ComSoc from 2018 to 2019, and the Vice President for Conferences of the IEEE France Section from 2017 to 2019. He is currently serving as a General Chair of WCNC 2021 and an Executive Co-Chair of GLOBECOM 2023. He served as an Editor for the IEEE Transactions on Communications from 1987 to 1991, an Associate Editor for the IEEE Communications Letters from 1999 to 2002, and a Guest Editor for several special issues of the IEEE Journal on Selected Areas in Communications, European Transactions on Telecommunications (ETT), and other journals. He served as a Distinguished Lecturer of ComSoc from 2001 to 2006, a member of the IEEE Fellow Evaluation Committee from 2002 to 2007, and a member of the IEEE Awards Committee from 2005 to 2007.